Received: 26 July 2023 | Revised: 24 October 2023 | Accepted: 28 November 2023

The Journal of Engineering

DOI: 10.1049/tje2.12338

The Institution of Engineering and Technology WILEY

LETTER

Energy harvesting from water flow through porous reduced graphene oxide networks

Reena A. Panchal[1] | **Nikhil A. Koratkar**[1,2]

[1]Department of Mechanical, Aerospace and Nuclear Engineering, Rensselaer Polytechnic Institute, Troy, New York, USA

[2]Department of Materials Science and Engineering, Rensselaer Polytechnic Institute, Troy, New York, USA

Correspondence
Nikhil A. Koratkar, Department of Mechanical, Aerospace and Nuclear Engineering, Rensselaer Polytechnic Institute, Troy, NY, USA.
Email: koratn@rpi.edu

Funding information
USA National Science Foundation, Grant/Award Number: 2002742

Abstract

Using a syringe pump setup, the authors conducted water flow experiments through porous reduced graphene oxide (rGO). A variety of anions and cations were added to the water to study its effect on energy harvesting. More specifically, the authors performed tests to study effect of: (1) ion concentration in water, (2) type of anion used, (3) type of cation used, and (4) effect of flow rate. The test data indicates that water flow through rGO networks can directly induce drift of charge carriers in graphene and thus generate electricity. Graphene is ideally suited for this application, since it possesses high mobility charge carriers that are ready to be coupled to moving ions present in the flowing fluid. The proposed rGO material could enable harvesting of the ubiquitous, abundant, and renewable mechanical energy of moving water directly to electrical energy. Unlike traditional schemes, the graphene material directly converts the flow energy into electrical energy without the need for moving parts. Such graphene coatings could potentially replace conventional batteries (which are environmentally hazardous) in low-power, low-voltage, and long service-life applications. Once scaled up, this concept offers a potentially transformative approach to energy harvesting, as opposed to incremental advances in current technologies.

1 | INTRODUCTION

It has been nearly two decades since Nobel Physics Laureates Andre Geim and Konstantin Novoselov first reported [1] using sticky tape to extract atomically thin layers of graphene from bulk graphite. Graphene, a single layer of carbon atoms bonded in a hexagonal lattice, is simultaneously the thinnest, strongest, and stiffest material found in nature, as well as being an excellent conductor of heat and electricity [2]. The extraordinary properties of graphene that have been reported in the literature [3–7] include its Young's modulus (~1100 GPa), fracture strength (125 GPa), thermal conductivity (~5000 W $m^{-1}K^{-1}$), mobility of charge carriers (200,000 cm^2 V^{-1} s^{-1}), and specific surface area (2630 m^2 g^{-1}) to name a few. Other interesting properties of graphene and 3D graphene networks have been reported including as photocatalysts [8, 9] and solar energy conversion applications [10].

The Nobel Physics prize to Geim and Novoselov has generated enormous interest within the scientific community to investigate the use of graphene for engineering applications. We discovered a potentially very exciting property of graphene, namely its ability to harvest electricity from flowing water [11]. When water flows over the graphene skin, ions present in water adsorb on to the graphene surface. Friction between the bulk flow and the adsorbed layer of ions causes the ions to acquire a net drift velocity (via stick-slip motion) in the flow direction on the graphene surface. Because of the sub-nm scale extreme thinness of the graphene sheets, the adsorbed surface ions exhibit a strong electrostatic coupling with the free charges that are present in the graphene sheets. The net result of this is that the free charge carriers in graphene are dragged along with the adsorbed surface ions in the flow direction resulting in an electric current and induced voltage generation in the fluid flow direction [11, 12].

Besides our work, many groups have reported similar observations of mV-level flow-induced voltage generation resulting from fluid-flow over graphene [13–15]. However, the majority of prior work to date has focused on water flow over individual graphene sheets deposited on insulating substrates. While such experiments are useful in terms of demonstrating the proof-of-concept and understanding the underlying mechanism, they are not practical for commercial applications due to the fragility of

the individual (monolayer) graphene sheet and the complexity associated with establishing high-quality electrical contacts with monolayer graphene. In this work, we explore a macroscopic and 3D reduced graphene oxide (rGO) network structure that is comprised of individual graphene sheets and show that water flow though this network can be used to successfully extract energy from the fluid flow. Such macroscopic and robust rGO materials can be manufactured [16, 17] in a scalable and cost-effective manner by top-down exfoliation of bulk graphite and show promise for practical applications.

2 | EXPERIMENTAL SECTION

2.1 | Synthesis of graphene oxide (GO) suspensions

GO powder (procured from ACS Materials) was dispersed in deionized (DI) water by ultrasonication with a concentration of ∼3 mg/mL in ∼20 mL batches. The dispersion was centrifuged at ∼14,000 rpm to remove multilayer species. The recovered supernatant is a solution of single-layer GO and is stable against precipitation for several months.

2.2 | Fabrication of free-standing GO films

Free-standing GO films were prepared by vacuum filtration of aqueous GO suspension through an Anodisc membrane filter (47 mm in diameter, 0.2 mm pore size; Whatman), followed by overnight drying in a vacuum desiccator. The resulting membrane was readily peeled off the filter paper, to yield a flexible free-standing film of GO. The as-prepared samples of free-standing GO were cut by a razor blade into rectangular strips of approximately 3.5 cm^2 area for testing without further modification.

2.3 | Reduction of GO to rGO films

Reduction of GO is an important processing step for this study. For this, ∼25 mL of hydrazine hydrate (Sigma Aldrich) was placed in an open ∼50 mL beaker in a vacuum desiccator. The freestanding film and GO drop-casted on quartz substrate was reduced for ∼30 h by exposure to hydrazine vapours under vacuum at room temperature to yield rGO films. Each piece was individually reduced, and upon removal from the desiccator, was characterized as is.

2.4 | Characterization of GO and rGO films

Figure 1a shows the diffraction pattern of the free-standing GO film that exhibits a narrow peak at $2\theta = 10.54°$ that corresponds to diffraction reflection from the (002) planes with the interlayer spacing of 8.25 Å. After the GO reduction, the (002) XRD-pattern diffraction peak has shifted to higher angles (Figure 1b) due to the decrease in the rGO interlayer spacing, which proves the reduction of oxygen-containing groups. The interlayer spacing of rGO has been determined to be 3.41 Å, which is consistent with the literature [18–20]. In case of GO, the small peak observed at approximately 20.1° indicates that a fraction of the GO is not fully interconnected with the oxygen atoms [21, 22]. In case of rGO, as the GO is reduced the distinct peak in GO reduces and becomes broader due to partial breakdown of long-range order of GO. Also, the peak position has slightly shifted towards a higher angle showing decrease in the lattice spacing. The weak peaks between 10° and 24° denote the coexistence of rGO and GO or partial reduction of GO [23]. The weak peak observed in the rGO spectra at approximately 6.5° can be due to the wet GO content in the sample. Since hydrazine hydrate vapours are used to reduce the GO sample, it is likely that the water vapour from the solution is absorbed in the sample. The rGO after reduction is not further processed by heating and so we believe that this peak indicates a small amount of wet GO in the sample [24].

Figures 2a and 2b show the survey XPS spectra of GO and rGO films respectively. High content of the oxygen-containing functional groups and low calculated C/O ratio (2.2) indicate that the GO is highly oxidized. After the reduction, the intensity of the C1s peak related to the oxidized groups decreases significantly, which is accompanied by a significant rise in the C/O ratio determined to be 4.524.

The thickness of the GO and rGO films was obtained from scanning electron microscopy (SEM) imaging of the fractured edge as shown in Figures 3a and 3b. The material thickness depends primarily on the concentration of the GO suspension that was used during the deposition. In our study, the GO concentration is ∼3 mg/mL, and in our case, the thickness of the GO and rGO films was observed to be ∼116 and ∼135 μm, respectively. The porous network structure of the rGO material is evident in the high-resolution SEM image provided in the inset of Figure 3b.

2.5 | Device fabrication and setup for flow transport experiments

For water transport experiments, the free-standing rGO films were placed on a clean glass substrate and silver electrodes were used as contact materials as shown in Figure 4a. Such a method of contacting the nanomaterial surface has been extensively used in the literature [25–32]. The fluid flow is along the longitudinal direction of the rGO film as indicated in Figure 4b. The rGO device is mounted at an angle so that the fluid can flow over it. The rate of fluid flow is accurately controlled by using a syringe pump (Figure 4b). The device was connected to a digital multi-meter to record the voltage generated during fluid flow. Voltage responses were measured in real time using a BenchVue data acquisition application. Note that the tip of the syringe pump is positioned such that the liquid does not contact the silver electrode and hence only contacts the rGO film. Thus, the generated voltages are not a result of electrochemical interaction between the contacts and water.

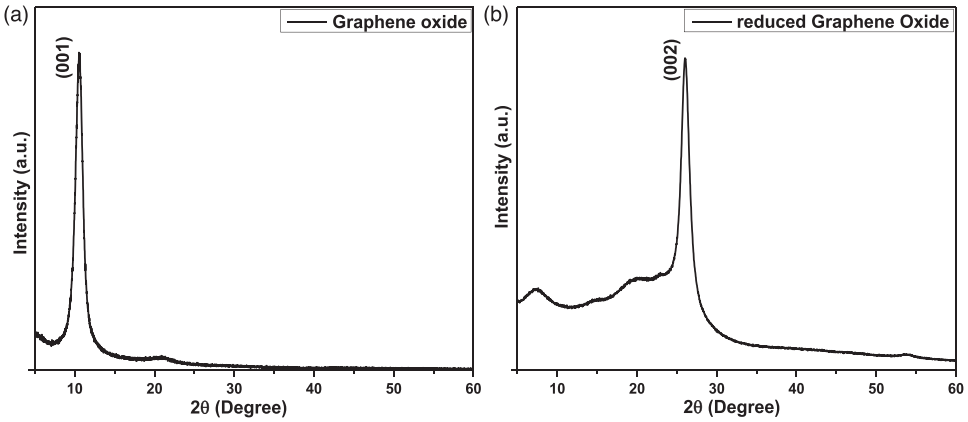

FIGURE 1 X-ray diffraction (XRD) patterns of free-standing (a) GO film, (b) reduced GO (rGO) film. Interlayer separation values for rGO are noticeably lower than the GO interlayer distance, which confirms reduction of interlayer water and oxygen-containing groups. GO, graphene oxide; rGO, reduced graphene oxide.

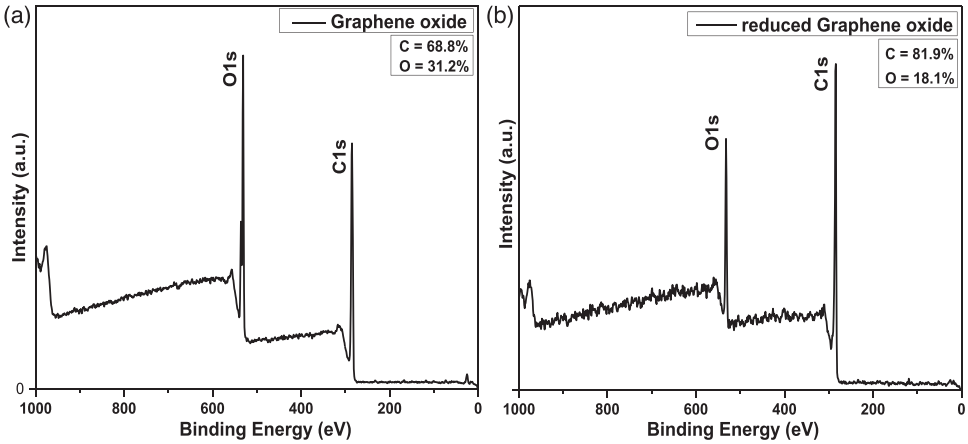

FIGURE 2 X-ray photoelectron spectroscopy (XPS) spectra of free-standing (a) GO film, (b) reduced GO film. There is substantial increase in carbon to oxygen ratio from GO to rGO, which confirms successful reduction. GO, graphene oxide; rGO, reduced graphene oxide.

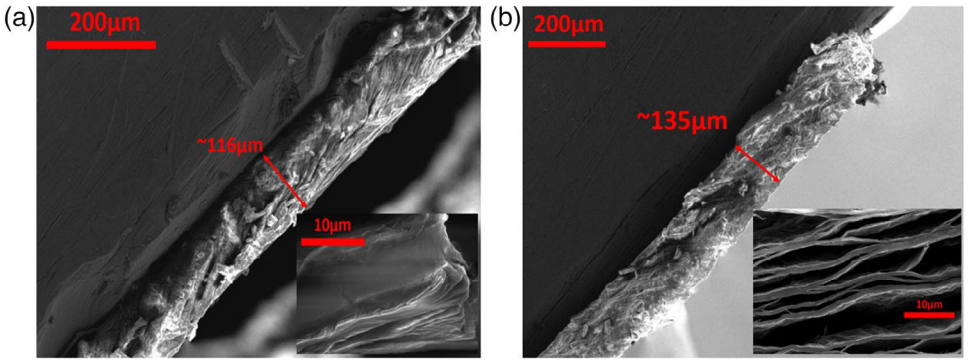

FIGURE 3 Scanning electron microscopy (SEM) of free-standing: (a) GO film (b) rGO film. Insets show zoom-in view of the porous network structure of these films. GO, graphene oxide; rGO, reduced graphene oxide.

2.6 | Effect of ion concentration

Water transport experiments with DI water yielded no appreciable voltage signal, which indicates that the presence of ions in the water is a necessary condition for the energy harvesting to take place. Tests were performed with different concentrations of potassium hydroxide (KOH) added to the water which results in K^+ cations and OH^- anions in the water. Flow-induced voltages in the rGO film are shown in Figure 5 for two different KOH concentrations namely 0.1 M and 0.5 M. The flow rate is held fixed at ~1 mL/Min in these tests. From the figure, we conclude the following:

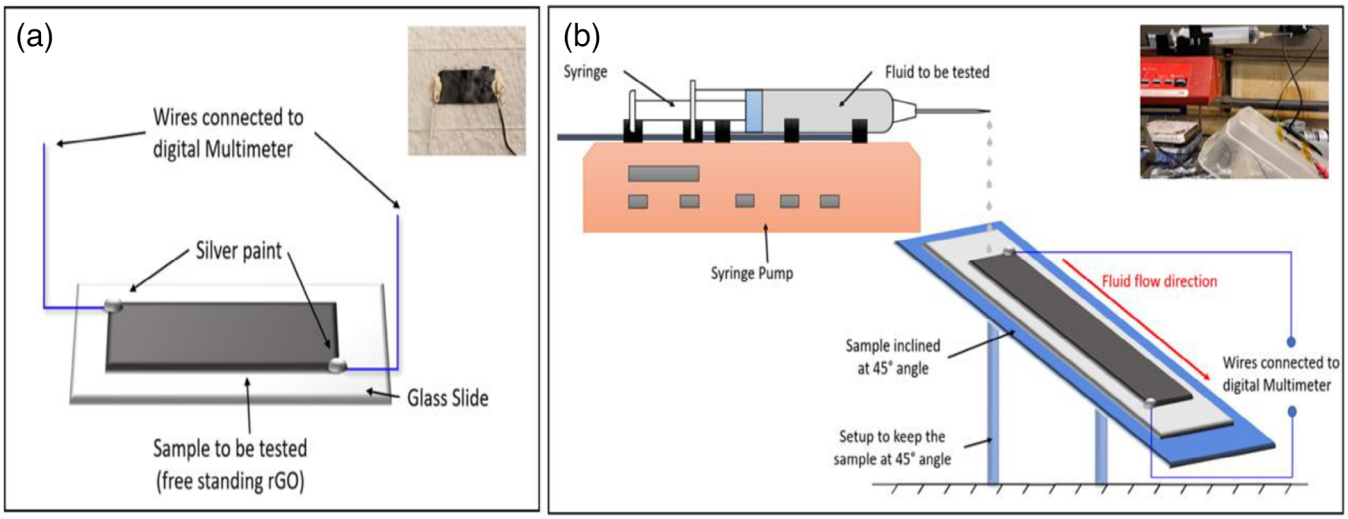

FIGURE 4 Schematic for (a) rGO device (inset: image of the sample); (b) setup for water flow experiments (inset: image of the setup). GO, graphene oxide; rGO, reduced graphene oxide.

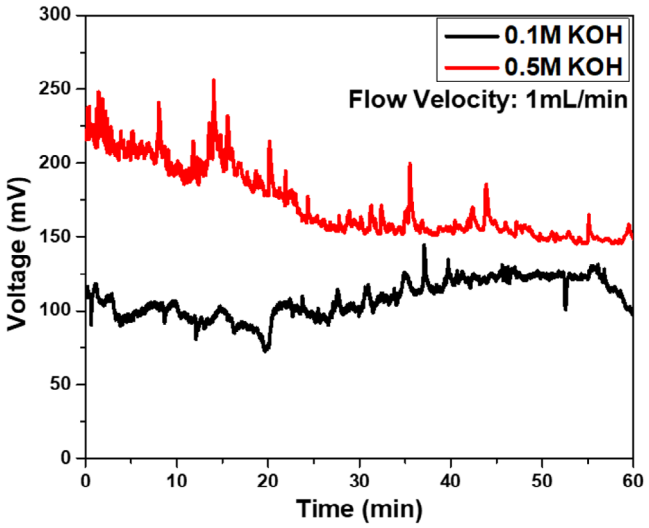

FIGURE 5 Effect of ion concentration on the energy-harvesting effect of rGO. rGO, reduced graphene oxide.

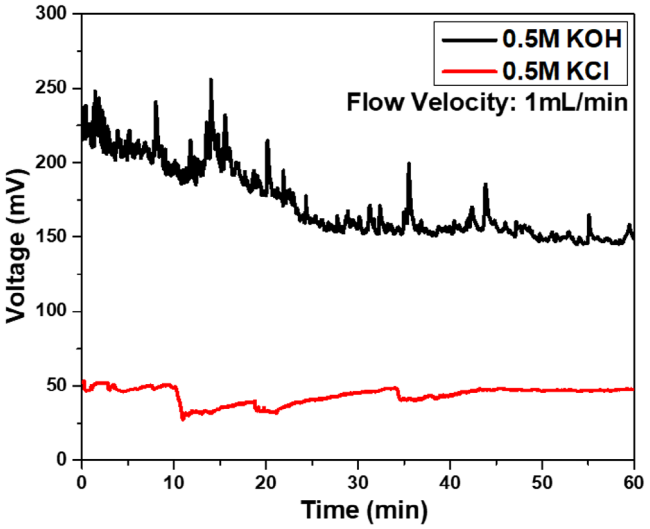

FIGURE 6 Effect of type of anion used on the energy-harvesting effect of rGO. rGO, reduced graphene oxide.

1. The flow-induced voltage in the rGO is strongly affected by the ion concentration, with a higher voltage generated at 0.5 M (~150 mV) when compared to 0.1 M (~120 mV).
2. The energy-harvesting effect is not a transient effect, since the power generation continued for over 60 min as indicated in the experiments.

2.7 | Effect of anion

In Figure 5, we report the effect of different OH^- anion concentrations on the energy-harvesting effect. We also decided to vary the type of anion. For this, we compared the performance of OH^- and Cl^- anions at the same concentration and with the same cation (K^+). To study this, flow transport experiments were conducted with KOH and potassium chloride (KCl) containing solutions at the same concentration of 0.5 M and at a fixed flow rate of ~1 mL/min. The test results are shown in Figure 6 and indicate that the anion has a strong effect on the voltage generation in the rGO film, with the OH^- anion performing much better than the Cl^- anion. These results indicate that the type of anion used has a powerful effect on the energy-harvesting performance.

2.8 | Effect of cation

Next, we studied whether the cation also plays a significant role in terms of harvesting energy from fluid flow. For this, we compared NaCl and KCl salts in the DI water. In this way, the anion

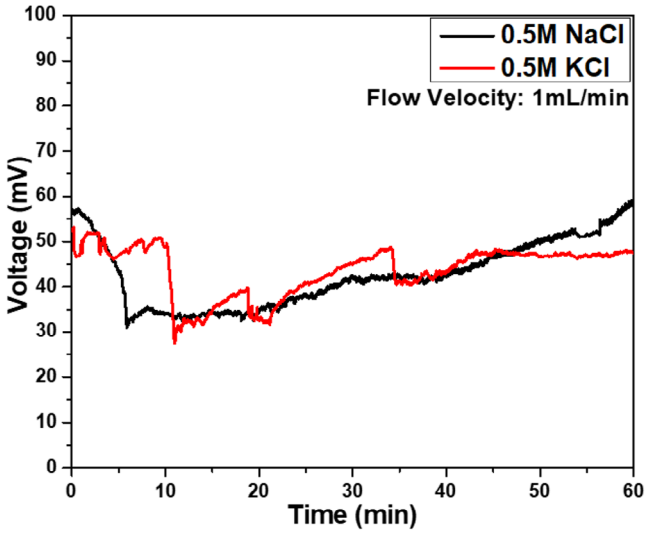

FIGURE 7 Effect of type of cation used on the energy-harvesting effect of rGO. rGO, reduced graphene oxide.

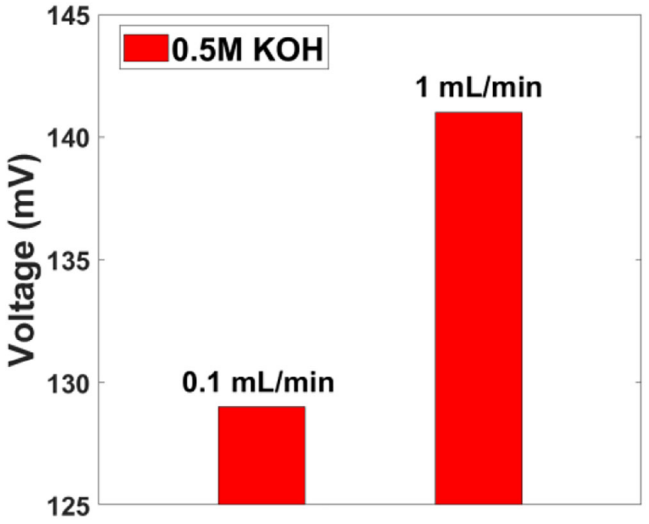

FIGURE 8 Effect of flow rate on the energy-harvesting effect of rGO films. rGO, reduced graphene oxide.

is the same (Cl^-) and only the cation (i.e. Na+ and K^+) is being varied. The flow velocity was fixed at ~1 mL/min and ion concentration was also fixed at ~0.5 M in these tests. The results (Figure 7) indicate that the type of cation has a weak effect on the energy-harvesting performance of the rGO film.

2.9 | Effect of flow rate

Finally, we studied the impact of flow rate on the energy harvesting effect. For this, we used K^+ as the cations and OH^- as the anions at a concentration of ~0.5 M. The experiments were performed at two different flow rates, namely ~0.1 and ~1 mL/min. The results indicate (Figure 8) that the increased flow rate improves the voltage generation effect.

TABLE 1 Comparison of our result with the literature for rGO-type films.

State-of-the-art flow-induced energy-harvesting results with rGO-type films	Open-circuit voltage	Ref.
Block copolymer-modified reduced graphene oxide	~19 mV	[33]
Reduced graphene oxide paper-pencil device	~280 mV	[34]
Reduced graphene oxide film	~ 1 mV	[35]
This study	~150 mV	

rGO, reduced graphene oxide.

3 | SUMMARY

In this letter, we report water flow experiments through porous rGO networks. The rGO materials are mechanically stable and can be manufactured by scalable top-down exfoliation methods. Based on our test results, we draw the following main conclusions:

- We find that the flow-induced voltage in the rGO is strongly affected by the ion concentration, with a higher voltage generated at higher ion concentrations.
- The energy-harvesting effect is not a transient (i.e. temporary) effect, since the power generation continued for over 60 min as indicated in the experiments.
- Our results indicate that the type of anion used has a powerful effect on the energy-harvesting performance. For example, OH^- anions perform much better than Cl^-.
- We find that the type of cation used has a weak effect on the energy-harvesting performance of the rGO film.
- The stronger effect of anions compared to cations indicates stronger coupling of anions with free charge carriers in the rGO material.
- Our results indicate that increased flow rate of the fluid flow greatly improves the voltage generation effect.

Table 1 compares our results with the literature [33–35] as it pertains to rGO-type materials. The rGO films tested here compare favourably with the literature. To conclude, we show that mechanical (flow) energy can be converted to electrical energy by flowing water (that contains ions) over rGO surfaces. The energy-harvesting mechanism uses stick-slip movement of ions on graphene surfaces to couple with free-charge carriers in graphene, and drag the charge carriers in the flow direction, resulting in an induced voltage. Hence, an increase in the fluid flow rate or the ion concentration increases the induced voltage. The anion has a stronger effect than the cation, presumably due to stronger coupling of anions with the free-charge carriers in graphene. Finally, we show that this mechanism is applicable not only to individual graphene sheets, but to rGO films, thus allowing energy to be harvested at a practically useful level.

CREDIT CONTRIBUTION STATEMENT

Reena A. Panchal synthesized the graphene materials and performed the energy harvesting experiments. Nikhil A. Koratkar

conceived and directed the project. Reena A. Panchal and Nikhil A. Koratkar wrote the manuscript.

CONFLICT OF INTEREST STATEMENT

The authors declare no conflict of interest.

FUNDING INFORMATION

The authors acknowledge support from the USA National Science Foundation (Award Number 2002742). Nikhil Koratkar also acknowledges support from the John A. Clark and Edward T. Crossan Chair Professorship at the Rensselaer Polytechnic Institute.

DATA AVAILABILITY STATEMENT

Data available on request from the authors.

ORCID

Nikhil A. Koratkar https://orcid.org/0000-0002-4080-3786

REFERENCES

1. Novoselov, K.S., Geim, A.K., Morozov, S.V., Jiang, D., Zhang, Y., Dubonos, S.V., Grigorieva, I.V., Firsov, A.A.: Electric field effect in atomically thin carbon films. Science 306, 666–669 (2004).
2. Park, S., Ruoff, R.S.: Chemical methods for the production of graphenes. Nat. Nanotechnol. 4, 217–224 (2009).
3. Noorden, R.V.: The trials of new carbon. Nature 469, 14–16 (2011).
4. Geim, A.K., Novoselov, K.S.: The rise of graphene. Nat. Mater. 6, 183–191 (2007).
5. Lee, C., Wei, X., Kysar, J.W., Hone, J.: Measurement of the elastic properties and intrinsic strength of monolayer graphene. Science 321, 385–388 (2008).
6. Van Den Brink, J.: Graphene: From strength to strength. Nat. Nanotechnol. 2, 199–201 (2007).
7. Li, D., Kaner, R.: Material science: Graphene-based materials. Science 320, 1170 (2008).
8. Zhang, F., Li, Y.-H., Li, J.-Y., Tang, Z.-R., Xu, Y.-J.: 3D graphene-based gel photocatalysts for environmental pollutants degradation. Environ. Pollut. 253, 365–376 (2019).
9. Zhang, N., Yang, M.-Q., Liu, S., Sun, Y., Xu, Y.-J.: Waltzing with the versatile platform of graphene to synthesize composite photocatalysts. Chem. Rev. 115, 10307–10377 (2015).
10. Han, C., Li, Y.-H., Qi, M.-Y., Zhang, F., Tang, Z.-R., Xu, Y.-J.: Surface/interface engineering of carbon-based materials for constructing multidimensional functional hybrids. Solar RRL 4, 1900577 (2020).
11. Dhiman, P., Yavari, F., Mi, X., Gullapalli, H., Shi, Y., Ajayan, P.M., Koratkar, N.: Harvesting energy from water flow over graphene. Nano Lett. 11, 3123–3127 (2011).
12. Petr, K., Shapiro, M.: Nanotube electron drag in flowing liquids. Phys. Rev. Lett. 86, 131 (2001).
13. Lee, S.H., Kang, Y.B., Jung, W., Kim, S., Noh, H.: Flow-induced voltage generation over monolayer graphene in the presence of herringbone grooves. Nanoscale Res. Lett. 8, 487 (2013).
14. Lee, S.H., Jung, Y., Kim, S., Han, C.S.: Flow-induced voltage generation in non-ionic liquids over monolayer graphene. Appl. Phys. Lett. 102, 063116 (2013).
15. Yin, J., Li, X.M., Yu, J., Zhang, Z.H., Zhou, J.X., Guo, W.L.: Generating electricity by moving a droplet of ionic liquid along graphene. Nat. Nanotechnol. 9, 378–383 (2014).
16. Huang, R., Huang, M., Li, X., An, F., Koratkar, N., Yu, Z.-Z.: Porous graphene films with unprecedented elastomeric scaffold-like folding behavior for foldable energy storage devices. Adv. Mater. 30, 1707025 (2018).
17. Park, S., Ruoff, R.S.: Chemical methods for the production of graphenes. Nat. Nanotechnol. 4, 217–224 (2009).
18. Bianco, A., Chen, Y., Chen, Y., Ghoshal, D., Hurt, R.H., Kim, Y., Koratkar, N., Meunier, V., Terrones, M.: A carbon science perspective in 2018: Current achievements and future challenges. Carbon 132, 785–801 (2018).
19. Gao, N., Fang, X.: Synthesis and development of graphene–inorganic semiconductor nanocomposites. Chem. Rev. 115, 8294–8343 (2015).
20. Peng, L., Hu, L., Fang, X.: Energy harvesting for nanostructured self-powered photodetectors. Adv. Funct. Mater. 24, 2591–2610 (2014).
21. Hsiao, M.-C., Liao, S.-H., Yen, M.-Y., Liu, P.-I., Pu, N.-W., Wang, C.-A., Ma, C.-C.M.: Preparation of covalently functionalized graphene using residual oxygen-containing functional groups. ACS Appl. Mater. Interfaces 2, 3092–3099 (2010).
22. Siburian, R., Sihotang, H., Raja, S.L., Supeno, M., Simanjuntak, C.: New route to synthesize of graphene nano sheets. Orient. J. Chem. 34, 182–187 (2018).
23. Huang, H.-H., De Silva, K.K.H., Kumara, G.R.A., Yoshimura, M.: Structural evolution of hydrothermally derived reduced graphene oxide. Sci. Rep. 8, 6849 (2018).
24. Lezzoche, A., Aixalà-Perelló, A., Pedico, A., Laurenti, M., Raffone, F., Lamberti, A.: Water flow-induced energy harvesting exploiting stacked graphene oxide membranes. Adv. Sustain. Syst. 7, 2300046 (2023).
25. Guler, O., Varol, T., Alver, U., Biyik, S.: The wear and arc erosion behavior of novel copper based functionally graded electrical contact materials fabricated by hot pressing assisted electroless plating. Adv. Powder Technol. 32, 2873–2890 (2021).
26. Chilkoor, G., Karanam, S.P., Star, S., Shrestha, N., Sani, R.K., Upadhyayula, V.KK, Ghoshal, D., Koratkar, N.A., Meyyappan, M., Gadhamshetty, V.: Hexagonal boron nitride: The thinnest insulating barrier to microbial corrosion. ACS Nano 12, 2242–2252 (2018).
27. Dubey, P.K., Sinha, A.S.K., Talapatra, S., Koratkar, N., Ajayan, P.M., Srivastava, O.N.: Hydrogen generation by water electrolysis using carbon nanotube anode. Int. J. Hydrogen Energy 35, 3945–3950 (2010).
28. Biyik, S.: Characterization of nanocrystalline $Cu_{25}Mo$ electrical contact material synthesized via ball milling. Acta Phys. Pol. A 132, 886–888 (2017).
29. Biyik, S., Arslan, F., Aydin, M.: Arc-erosion behavior of boric oxide-reinforced silver-based electrical contact materials produced by mechanical alloying. J. Electron. Mater. 44, 457–466 (2015).
30. Wang, D., Yang, A., Lan, T., Fan, C., Pan, J., Liu, Z., Chu, J., Yuan, H., Wang, X., Rong, M., Koratkar, N.: Tellurene based chemical sensor. J. Mater. Chem. A 7, 26326–26333 (2019).
31. Biyik, S.: Influence of type of process control agent on the synthesis of Ag_8ZnO composite powder. Acta Phys. Pol. A 135, 778–781 (2019).
32. Biyik, S.: Effect of cubic and hexagonal boron nitride additions on the synthesis of Ag–SnO2 electrical contact material. J. Nanoelectron. Optoelectron. 14, 1010–1015 (2019).
33. Daripa, S., Khawas, K., Behere, R.P., Verma, R., Kuila, B.K.: Efficient moisture-induced energy harvesting from water-soluble conjugated block copolymer-functionalized reduced graphene oxide. ACS Omega 6, 7257–7265 (2021).
34. Aruna, R.K., Singha, P., Biswasb, G., Chandaa, N., Chakraborty, S.: Energy generation from water flow over reduced graphene oxide surface in a paper-pencil device. Lab Chip 16, 3589–3596 (2016).
35. Wang, K., Liu, Y., Li, J., Li, J.: Electricity generation as ionic solution droplet sliding on a self-assembled reduced graphene oxide film. J. Mater. Chem. A 8, 12735–12743 (2020).

How to cite this article: Panchal, R.A., Koratkar, N.A.: Energy harvesting from water flow through porous reduced graphene oxide networks. J. Eng. 2024, 1–6 (2024). https://doi.org/10.1049/tje2.12338